physica p s s status solidi

physica **p s s** status solidi ^c

current topics in solid state physics

Ground State of Electron-Hole Bilayer
Kazuo Yamashita, Kenichi Asano,
Takuma Ohashi

physica **p s s** status solidi ^b

www.pss-b.com
basic solid state physics

New article series

Advanced Calculations
for Defects in Materials –
Electronic Structure
Methods

Feature Article
Chris G. Van de Walle
and Anderson Janotti

physica **p s s** status solidi ^a

www.pss-a.com
applications and materials science

Expert Opinion
Solid-state lighting
Roland Haitz and Jeffrey Y. Tsao

WILEY-VCH

physica **p s s** status solidi ^{rrl}

www.pss-rapid.com
rapid research letters

New: review@rrl

Competing energy scales in
high-temperature superconductors:
Ultrafast pump-probe studies
Elbert E. M. Chia, Jian-Xin Zhu,
D. Talbayev, and A. J. Taylor

WILEY-VCH

WILEY-VCH

physica **pss** status solidi a
www.pss-a.com
applications and materials science

Effect of the *pn* junction engineering on Si microwire-array solar cells

A. Dalmau Mallorquí, F. M. Epple, D. Fan, O. Demichel, and A. Fontcuberta i Morral*

Laboratoire des Matériaux Semiconducteurs, École Polytechnique Fédérale de Lausanne, 1015 Lausanne, Switzerland

* Corresponding author: e-mail anna.fontcuberta-morral@epfl.ch, Phone: +41-21-6937394, Fax: +41-21-6934755

We report on the impact of the doping concentration design on the performance of silicon microwire arrays as photovoltaic devices. We have fabricated arrays with different *p*- and *n*-doping profiles and thicknesses, obtaining mean efficiencies as high as 9.7% under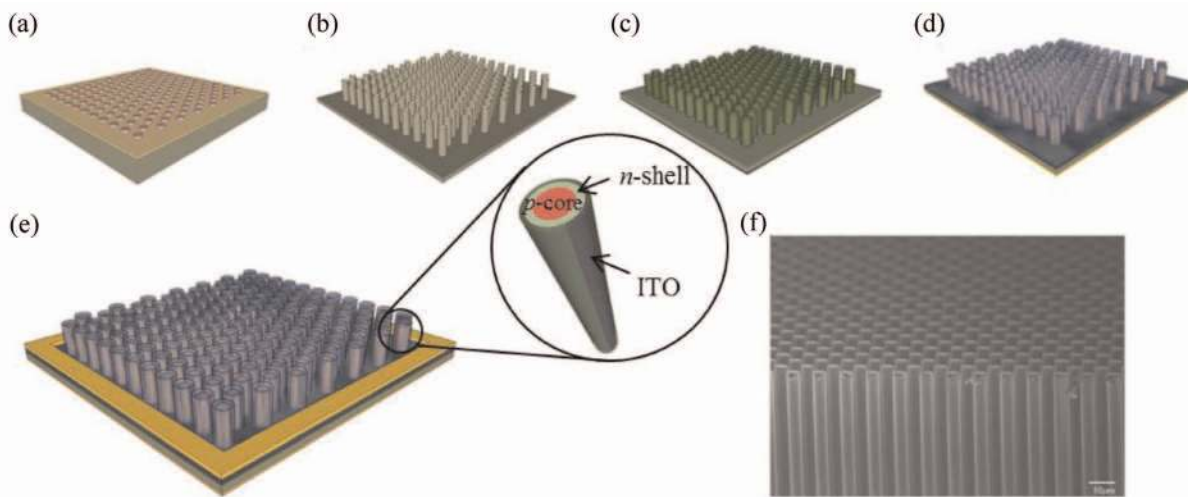 AM 1.5G solar illumination. The results reveal the importance of scaling the microwire diameter with the depletion width resulting from doping concentrations. The doping of the core should be kept low in order to reduce bulk recombination. Furthermore, the thickness of the *n*-shell should be kept as thin as possible to limit the emitter losses.

© 2012 WILEY-VCH Verlag GmbH & Co. KGaA, Weinheim

1 Introduction Photovoltaic production and research has grown exponentially over the last twenty years due to the rising economic and environmental cost of fossil fuels. However, the cost per unit of energy produced remains high compared to typical grid prices. Thus, new concepts and technologies are arising to increase the efficiency/cost ratio [1]. Within this framework, nanowire-based *p–n* radial junctions constitute a promising approach. By enhancing light trapping over a wide range of wavelengths and decoupling the direction of light absorption and carrier collection, these architectures can improve the efficiency of photovoltaic devices and ease the quality requirements of the materials of which they are composed [2, 3]. Recent studies in Si nanowires have reported efficiencies up to 9% for single-wire devices [4] and 11% for an array of vertical wires [5]. Nanowire-based devices offer scope for further improvement by increasing light absorption (either by changing the wire geometry and the array configuration [6–9] or adding scattering nanoparticles between the wires [10]) or by decreasing the surface recombination via surface passivation [5, 11].

In the present work, we study how the particular design of a radial *pn* junction affects the light conversion efficiency of the device. For this, we vary the microwire diameter, doping concentrations and junction depth. The results are evaluated by measuring the conversion efficiency under AM 1.5 conditions and the external quantum efficiency (EQE).

2 Experimental details A scheme of the solar cell fabrication process is shown in Fig. 1. Ordered arrays of microwires are fabricated by a combination of optical lithography and deep reactive ion etching on a 380 µm thick Czochralski ⟨100⟩ *p*-doped Si wafer [12]. Hexagonally packed 45-µm long wires with diameters of 1.86, 2.4, and 3.1 µm, spaced 7, 8, and 10 µm, respectively, are obtained. Three substrates with different resistivities are used: 0.1–0.5, 1–5, and 1–10 Ω cm. The *n*-shell is formed by diffusing POCl₃ for 15 min at 850 and 900 °C. In order to diminish the defect concentration at the surface of the wires caused by the etching process, a thermal oxidation step is added right after the diffusion. The oxide layer is stripped off by wet etching in HF. A conformal indium tin oxide (ITO) layer with a nominal thickness of 70 nm is sputtered on the front side as an *n*-contact and 200 nm of Al as a rear contact. Optical and electrical properties of ITO were measured with an ellipsometer (Sopra GES-5E) and a resistivity meter four-point measurements, respectively, obtaining a transmittance in the visible range of 96% and a resistivity of 0.2–0.4 mΩ cm, which proves ITO as a suitable front contact. In order to get a better contact for electrical measurements, four Ti/Au pads (10/200 nm) are evaporated around the array. The surface of the arrays is 5.4 × 5.4 mm². A scanning electron microscopy (SEM) image of a typical array is shown in Fig. 1f. Wires are uniform in diameter along the whole length and across de wafer.

© 2012 WILEY-VCH Verlag GmbH & Co. KGaA, Weinheim

Original

Paper

Phys. Status Solidi A 209, No. 8 (2012)   1589

Figure 1 (online color at: www.pss-a.com) Fabrication schematic of radial p–n junction Si microwire arrays: (a) patterning of a p-type Si wafer by means of photolithography; (b) deep reactive ion etching to obtain p-core microwire arrays; (c) POCl$_3$ diffusion to create an n-shell; (d) ITO and Al sputtering as front and rear contacts, respectively; and (e) evaporation of Ti/Au contacts around the arrays. A detail of the resulting cross-section is also depicted. (f) SEM image of a fabricated microwire array viewed at $\sim$30° tilt.

3 Results and discussion The doping concentration profiles of the junctions were measured by capacitance–voltage measurements (Wafer Profiler CVP21) on flat substrates exposed to the same diffusion treatments. The results transposed to the wire pn junctions are shown in Fig. 2 (the erratic profile of the p-doped region is due to an experimental aberration resulting from the sharpness of the junction [13]). As expected from the fabrication process, the doping concentration of the core is constant, while the doping concentration at the shell decreases from the surface to the core following the diffusion profile depicted by Fick's law [14]:

$$\frac{\partial N_D}{\partial t} = D\frac{\partial^2 N_D}{\partial x^2},$$

where N_D is the dopant concentration, D is the diffusivity of P into Si, t is the diffusion time and x the diffusion depth. As shown in Fig. 2, the fitting of the doping profiles for a diffusion of POCl$_3$ at 850 °C and 35 min (corresponding to the continuous lines) are in agreement with CV measurements. In order to understand the effect of the doping profiles on the transition between the n- and p-regions, we have calculated the depletion width in both regions by solving Poisson's equation at the junction. Assuming the continuity of the electric field ξ at the junction and fixing the differential potential between the n and p regions to be equal to the built-in voltage (V_{bi}) yields [15]

$$\frac{1}{K_s\varepsilon_0}\int_{x_j}^{x_n}\rho(x)dx = \frac{1}{K_s\varepsilon_0}\int_{-x_p}^{x_j}\rho(x)dx$$

$$V_{bi} = -\int_{-x_p}^{x_n}\xi(x)dx,$$

where K_s is the relative dielectric constant, $\varepsilon_0 = 8.854 \times 10^{-14}$ (F/cm), ρ the net charge density, x_j the

junction depth, and x_n and x_p denote the depletion limits. The depletion widths resulting from these calculations are reported in Table 1 and indicated by gray areas in Fig. 2. The plot shows the microwire cross-section with the doping
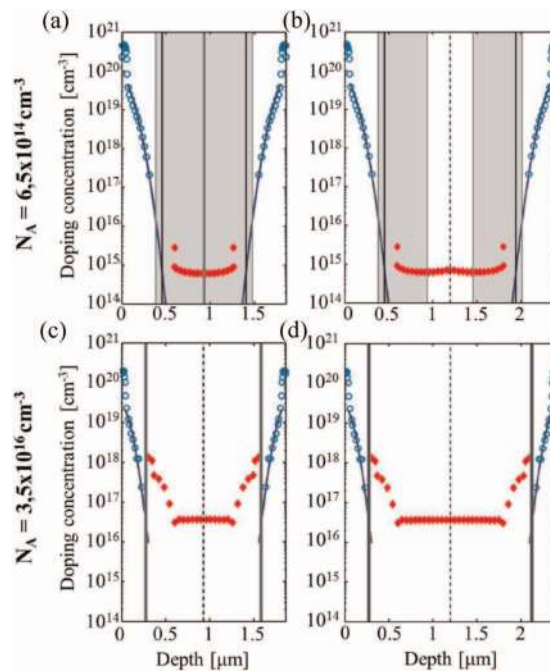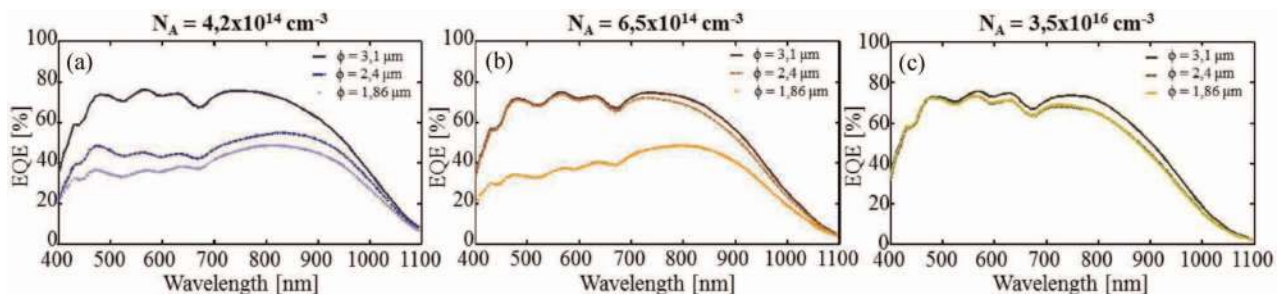

Figure 2 (online color at: www.pss-a.com) Doping profiles across the wire cross-section. The symbols represent experimental measurements and the continuous lines show the simulated diffusion profiles. Vertical black lines define the position of the junction, while gray areas represent depleted regions for four different situations: (a) $N_A = 6.5 \times 10^{14}$ cm^{-3}, $\phi = 1.86$ μm; (b) $N_A = 6.5 \times 10^{14}$ cm^{-3}, $\phi = 2.4$ μm; (c) $N_A = 3.5 \times 10^{16}$ cm^{-3}, $\phi = 1.86$ μm; (d) $N_A = 3.5 \times 10^{16}$ cm^{-3}, $\phi = 2.4$ μm.

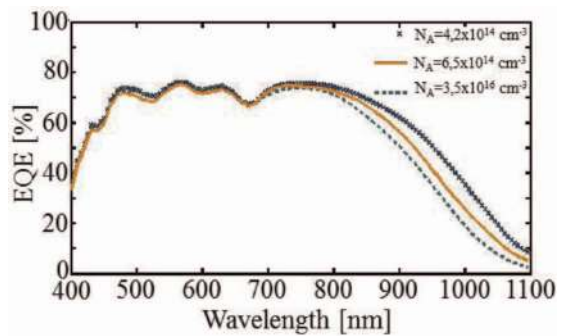**Table 1** Average measured properties of solar cell devices.

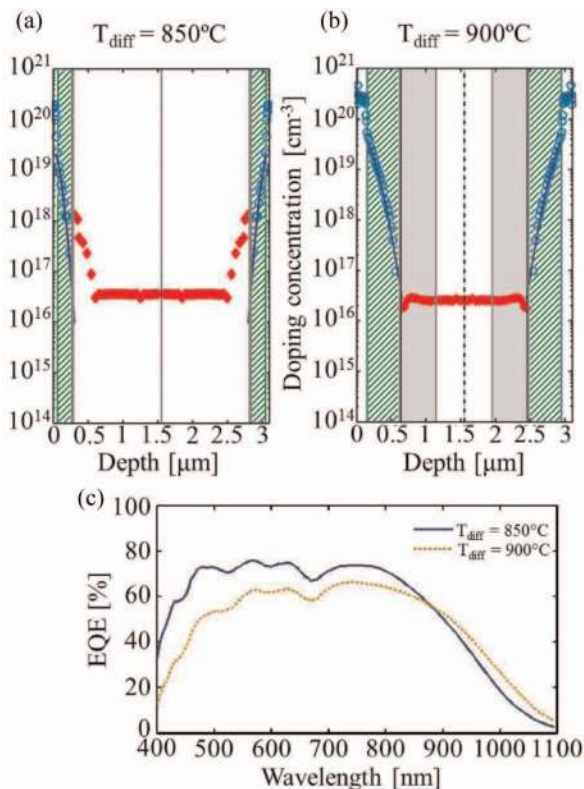| ϕ (μm)	N_A (cm^{-3})	depletion width (nm)	J_{sc} (mA/cm^2)	V_{oc} (V)	FF	η (%)
1.86	4.2×10^{14}	758	20.0	0.53	0.74	7.9
	6.5×10^{14}	555	19.8	0.55	0.71	7.7
	3.5×10^{16}	77	22.3	0.54	0.58	6.9
2.40	4.2×10^{14}	758	21.6	0.53	0.73	8.4
	6.5×10^{14}	555	23.3	0.53	0.64	7.9
	3.5×10^{16}	77	22.4	0.54	0.57	6.8
3.10	4.2×10^{14}	758	24.9	0.53	0.74	9.7
	6.5×10^{14}	555	24.4	0.54	0.68	9.0
	3.5×10^{16}	77	22.7	0.50	0.50	5.8
planar	4.2×10^{14}	758	18.9	0.53	0.76	7.6
	6.5×10^{14}	555	20.3	0.55	0.74	8.3
	3.5×10^{16}	77	17.9	0.55	0.62	6.1

Figure 4 (online color at: www.pss-a.com) Comparison of the EQE of microwire arrays for the three different *p*-doping concentrations: 4.2×10^{14}, 6.5×10^{14}, and 3.5×10^{16} cm^{-3}. The diameter of the wires is 3.1 μm in the three cases.

profiles and the depletion region widths for two different *p*-doping concentrations (6.5×10^{14} and 3.5×10^{16} cm^{-3}) and two wire diameters (1.86 and 2.4 μm). Comparing these two cases, we observe that wires with higher *p*-doping concentration present thinner depletion widths (77 nm compared to 555 nm) and shallow junction depths (270 nm instead of 455 nm). As a consequence, for the smallest diameter nanowires (1.86 μm) the core is fully depleted. This effect occurs for diameters of 1.86 and 2.4 μm when the *p*-doping concentration is 4.2×10^{14} cm^{-3} and for a diameter of 1.86 μm in the case of a *p*-doping concentration of 6.5×10^{14} cm^{-3}.

We study the effect of the depletion width and wire diameter on the performance of the device. EQEs for all the *pn* junction designs are compared in Fig. 3. As shown in plots (a) and (b) of Fig. 3, for small diameters and low *p*-doping concentrations EQE decreases dramatically, especially in the visible regime as the light is mainly absorbed in the wires. For long wavelengths, where photons are absorbed beneath the wires [16], the EQE for all the diameters becomes similar. The solar power conversion efficiencies were also measured under an AM 1.5G illumination, obtaining a maximum mean efficiency of 9.7%. All the results summarized in Table 1 were averaged over four samples fabricated under identical conditions. They show that fill factor (FF) and efficiency (η) both increase with decreasing the *p*-doping concentration.

This improvement is mainly due to a decrease of the recombination at the bulk [17]. To further illustrate this, we compare the EQE curves of arrays with a wire diameter of 3.1 μm and different *p*-doping (Fig. 4). Clearly, long wavelength photons, which are absorbed in the bulk, are collected more efficiently in the case of low doping concentrations of the substrate. These measurements also indicate that the larger is the not depleted core, the higher is the short-circuit current density, presumably as a result of increased carrier collection. It should be noted that this statement can only be true as long as the distance from the center of the nanowire to the depletion region is smaller than the diffusion length of the minority carriers.

Finally, we examine the solar cell performance for different doping concentrations of the shell. For this, we keep the doping of the substrate constant to 3.5×10^{16} cm^{-3} and vary the *n*-type doping by diffusing POCl$_3$ at two different temperatures: 850 and 900 °C. The *n*-doping profiles for these two cases are shown in Fig. 5a and b. As the mobility of dopants increases with the temperature, the *pn* junction is formed at 270 nm from the surface in the case of a diffusion at 850 °C and at 635 nm for a diffusion at 900 °C. In the first case, the doping concentration decreases more abruptly.

To evaluate the collection efficiency of photogenerated carriers, we need to take into account the minority diffusion lengths of the carriers, which depends on the carrier

Figure 3 (online color at: www.pss-a.com) EQE as function of the diameter for (a) $N_A = 4.2 \times 10^{14}$ cm^{-3}, (b) $N_A = 6.5 \times 10^{14}$ cm^{-3}, and (c) $N_A = 3.5 \times 10^{16}$ cm^{-3}.

Phys. Status Solidi A 209, No. 8 (2012)
1591

Original

Paper

Figure 5 (online color at: www.pss-a.com) Doping profiles across the wire cross-section for a diffusion temperature of (a) 900 °C and (b) 850 °C. The symbols represent experimental measurements and the continuous lines show the simulated diffusion profiles. Vertical black lines define the position of the junction, gray areas represent depleted regions and shaded green areas depict the zone where the diffusion length of minority carriers is higher than the distance to the junction. (c) Comparison of the EQE when changing the doping profile of the shell.

4 Conclusions In summary, we have demonstrated the influence of the *pn* junction design on the carrier collection and electrical conversion efficiency. The minimum diameter of the wires is limited by the width of the depletion region resulting from the *p*- and *n*-doping concentrations. Moreover, the junction should be as close as possible to the side facets surface.

References

 [1] M. A. Green, Prog. Photovolt.: Res. Appl. **9**, 123–135 (2001).
 [2] B. M. Kayes, H. A. Atwater, and N. S. Lewis, J. Appl. Phys. **97**(11), 114302 (2005).
 [3] R. R. LaPierre, J. Appl. Phys. **109**(3), 034311 (2011).
 [4] M. D. Kelzenberg, D. B. Turner-Evans, D. B. Kayes, B. M. Filler, M. C. Putnam, N. S. Lewis, and H. A. Atwater, Single-nanowire Si solar cells, in: Proc. 33rd IEEE Photovoltaic Spec. Conf., San Diego, CA, 2008.
 [5] D. R. Kim, C. H. Lee, P. M. Rao, I. S. Cho, and X. L. Zheng, Nano Lett. **11**, 2704–2708 (2011).
 [6] M. D. Kelzenberg, S. W. Boettcher, J. A. Petykiewicz, D. B. Turner-Evans, M. C. Putnam, E. L. Warren, J. M. Spurgeon, R. M. Briggs, N. S. Lewis, and H. A. Atwater, Nature Mater. **9**, 239–244 (2010).
 [7] M. Foldyna, L. Yu, B. O'Donnell, and P. R. i. Cabarrocas, Optical absorption in vertical silicon nanowires for solar cell applications, in: Proc. SPIE, 2011.
 [8] J. Kupec, R. L. Stoop, and B. Witzigmann, Opt. Express **18**(26), 27589–27605 (2010).
 [9] J. Zhu, Z. Yu, G. F. Burkhard, C. M. Hsu, S. T. Connor, Y. Xu, Q. Wang, M. McGehee, S. Fan, and Y. Cui, Nano Lett. **9**, 279–282 (2009).
[10] M. C. Putnam, S. W. Boettcher, M. D. Kelzenberg, D. B. Turner-Evans, J. M. Spurgeon, E. L. Warren, R. M. Briggs, N. S. Lewis, and H. A. Atwater, Energy Environ. Sci. **3**, 1037–1041 (2010).
[11] M. D. Kelzenberg, D. B. Turner-Evans, M. C. Putnam, S. W. Boettcher, R. M. Briggs, J. Y. Baek, N. S. Lewis, and H. A. Atwater, Energy Environ. Sci. **4**, 866–871 (2011).
[12] C. Kendrick, H. Yoon, Y. Yuwen, G. Barber, H. Shen, T. Mallouk, E. Dickey, T. Mayer, and J. Redwing, Appl. Phys. Lett. **97**(14), 143108 (2010).
[13] W. C. Johnson and P. T. Panousis, IEEE Trans. **ED-18**, 965–973 (1971).
[14] S. W. Jones, Diffusion in Silicon (IC Knowledge LLC, Georgetown, MA, 2008).
[15] G. W. Neudeck, The pn Junction Diode (Addison-Wesley Publ. Co., Reading, MA, 1989).
[16] M. A. Green and M. J. Keevers, Prog. Photovolt.: Res. Appl. **3**, 189–192 (1995).
[17] D. Macdonald and A. Cuevas, Prog. Photovolt.: Res. Appl. **8**, 363–375 (2000).
[18] J. del Alamo, S. Swirhun, and R. M. Swanson, Solid-State Electron. **28**, 47–54 (1985).

concentration [18]. The diffusion length of holes at an electron concentration of 2×10^{20} cm^{-3} (doping concentration at the surface) is as low as 200 nm, meaning that carriers generated at the surface cannot be collected as the beginning of the depletion area is 627 nm deep for a diffusion of 900 °C. Shaded green areas in Fig. 5a and b correspond to the regions where the photogenerated carriers can be efficiently collected. This area is remarkably closer to the nanowire surface for the lower temperature diffusion (around 60 nm) than for the higher one (around 150 nm). Now we compare this with the spectral dependence of the EQE of the device (Fig. 5c). The cells obtained with an 850 °C diffusion exhibit a higher EQE in a wider range of wavelengths, and especially in the visible regime. This result is in agreement with the existence of a smaller region in the nanowire over which the photogenerated carriers cannot be collected, giving rise to fewer recombination losses in the emitter region. This translates into a 4.6% higher J_{sc} for cells with *n*-doped layers obtained by an 850 °C diffusion (22.73 mA/cm^2) compared to those diffused at 900 °C (21.73 mA/cm^2).